A Role of Erythrocytes in Adenosine Monophosphate Initiation of Hypometabolism in Mammals*[S]

Isadora Susan Daniels[‡1,2], **Jianfa Zhang**[‡§1,3], **William G. O'Brien III**[‡], **Zhenyin Tao**[‡], **Tomoko Miki**[‡], **Zhaoyang Zhao**[‡], **Michael R. Blackburn**[‡], **and Cheng Chi Lee**[‡4]

From the [‡]*Department of Biochemistry and Molecular Biology, University of Texas Health Science Center, Houston, Texas 77030 and the* [§]*Center for Molecular Metabolism, Nanjing University of Science and Technology, Nanjing 210094, China*

Biochemical and mechanistic aspects into how various hypometabolic states are initiated in mammals are poorly understood. Here, we show how a state of hypometabolism is initiated by 5′-AMP uptake by erythrocytes. Wild type, ecto-5′-nucleotidase-deficient, and adenosine receptor-deficient mice undergo 5′-AMP-induced hypometabolism in a similar fashion. Injection of 5′-AMP leads to two distinct declining phases of oxygen consumption (VO_2). The phase I response displays a rapid and steep decline in VO_2 that is independent of body temperature (T_b) and ambient temperature (T_a). It is followed by a phase II decline that is linked to T_b and moderated by T_a. Altering the dosages of 5′-AMP from 0.25- to 2-fold does not change the phase I response. For mice, a T_a of 15 °C is effective for induction of DH with the appropriate dose of 5′-AMP. Erythrocyte uptake of 5′-AMP leads to utilization of ATP to synthesize ADP. This is accompanied by increased glucose but decreased lactate levels, suggesting that glycolysis has slowed. Reduction in glycolysis is known to stimulate erythrocytes to increase intracellular levels of 2,3-bisphosphoglycerate, a potent allosteric inhibitor of hemoglobin's affinity for oxygen. Our studies showed that both 2,3-bisphosphoglycerate and deoxyhemoglobin levels rose following 5′-AMP administration and is in parallel with the phase I decline in VO_2. In summary, our investigations reveal that 5′-AMP mediated hypometabolism is probably triggered by reduced oxygen transport by erythrocytes initiated by uptake of 5′-AMP.

Mammals in deep hypometabolism (DH)[5] with severe hypothermia and stupor are only observed naturally during hibernation (1). During hibernation, an animal's overall metabolic rate, based on oxygen consumption, is a small fraction of its euthermic needs. The biochemical event that triggers this hypometabolism is an enigma. It is thought that non-hibernating mammals cannot undertake a similar hypometabolic process because

deep hypothermia is often associated with ventricular fibrillation and cardiac arrest.

However, organs from non-hibernators can withstand a considerable ischemic period in a hypometabolic state. For example, during human organ transplantation, donated organs are transported in a cold ischemic state in the complete absence of blood circulation for many h (2), yet when implanted into a recipient, the restoration of blood flow and rewarming revives full organ function. This phenomenon also illustrates the important role of oxygen transportation by erythrocytes in metabolic activity. In addition, observations that exsanguination and prolonged hypoxia can result in hypothermia further demonstrate the importance of oxygen transportation and availability as factors that can modulate the metabolic rate in mammals (3, 4).

We have demonstrated that the metabolite 5′-AMP can induce mice to undergo transient hypometabolism with T_b as low as 26 °C, similar to a torpor-like state (5). The T_b of animals in torpor is defined to be at or moderately below 31 °C (6). Here, we demonstrate that 5′-AMP under the appropriate T_a can also be used to induce a reversible DH in which VO_2 levels are less than 10% of normal euthermic demand. Our studies reveal that the 5′-AMP-mediated DH is accompanied by two distinct phases of VO_2 decline. Immediately following 5′-AMP administration, the phase I decline in VO_2 is steep, rapid, and independent of both T_b and T_a. This is followed by a gradual phase II decline that is moderated by T_a and T_b. Although our investigations show that erythrocytes take up 5′-AMP and use ATP to convert it to ADP, the majority of the 5′-AMP is rapidly catabolized. The uptake of 5′-AMP coincides with a rise in 2,3-bisphosphoglycerate (2,3-BPG) levels produced by the erythrocytes. The rise in 2,3-BPG is consistent with the observed phase I response because 2,3-BPG is a potent allosteric inhibitor of hemoglobin's affinity for oxygen. Spectral analysis of blood obtained from mice shortly after 5′-AMP administration revealed increased levels of deoxyhemoglobin.

EXPERIMENTAL PROCEDURES

Animals—These studies primarily used female mice (C57Bl/6), aged between 8 and 16 weeks. Mice were housed in a standard animal facility under a 12-h/12-h light/dark cycle with T_a between 22 and 24 °C. Male Sprague-Dawley rats weighing between 450 and 550 g were housed in similar facilities. All mouse studies were carried out under institutionally approved animal protocols HSC-AWC-06-078 (University of Texas Health Science Center) and NWC-06-039 (Nanjing University

of Science and Technology). Rat experiments were undertaken with institutionally approved animal protocol HSC-AWC-07-046 (University of Texas Health Science Center). Dog experiments were undertaken with institutionally approved animal protocol NWC-06-039 (Nanjing University of Science and Technology). Care and use of animals for this study were in compliance with relevant animal welfare guidelines approved by the Animal Welfare Committee at the University of Texas Health Science Center.

DH Methods—Each mouse was injected intraperitoneally with the appropriate dosages of freshly prepared 5′-AMP (Sigma catalogue no. A1752-25G) dissolved in phosphate-buffered saline. For routine induction of DH, mice received 0.5 mg/g 5′-AMP and were maintained at 15 °C T_a throughout the entire procedure. Physical interaction with the animals was kept to a minimum once 5′-AMP had been administered. For rapid cooling, mice were given 0.125–0.5 mg/g of 5′-AMP and were kept at 4 °C for about 1 h before being transferred to a T_a of 15 °C. Core body temperature was measured by telemetry, using a G2 E-mitter (Columbus Instruments and Mini-Mitter Respironics). Oxygen consumption and carbon dioxide production rates were measured in an environmentally controlled comprehensive laboratory animal monitoring system (Columbus Instruments). Respiration rate was determined by counting the number of inhalations and exhalations over 10-s intervals. Heart rate and body temperature were measured with a mouse THM100 temperature and ECG monitoring system (Indus Instruments). Body temperature was manually monitored by a digital thermometer (Traceable, Fisher; catalogue no. 15-077-8) placed into the rectum.

Erythrocyte Uptake of [^{14}C]Adenosine or 5′-[^{14}C]AMP—Erythrocytes were isolated by differential centrifugation (1000 × g) from heparinized mouse blood, washed in a 2× volume of ice-cold PBS (four times), followed by ice cold Hanks' buffered salt solution (two times) with the final volume equal to the original blood volume. 1 μl of [^{14}C]adenosine (43 mCi/mmol and 100 μCi/ml) or 5′- [^{14}C]AMP (50 mCi/mmol and 100 μCi/ml) was mixed with 50 μl of erythrocytes and centrifuged either immediately or after incubation at 37 °C for 60 min. The supernatant was removed, and the erythrocyte pellet was washed with 1 ml of Hanks' buffered salt solution and repelleted. The pellet was treated with 50 μl of 10% trichloroacetic acid, and the supernatant was separated from insoluble products by centrifugation. Erythrocyte uptake of [^{14}C]adenosine or 5′-[^{14}C]AMP was determined by analyzing 10 μl of the supernatant in 10 ml of scintillant using a LKG 1209 counter. Products containing ^{14}C were identified by TLC (Silica Gel 60 F$_{254}$, EMD Chemicals, Inc.) in solvent containing butanol/methanol/water/ammonium hydroxide (60:20:19:1). All ^{14}C-labeled nucleotides were obtained from GE Healthcare. The ^{14}C-labeled nucleosides were obtained from MP Biomedicals. Levels of 2,3-BPG in erythrocytes were measured using a kit (Roche Applied Science). Hemoglobin content was determined by an automated hematology analyzer (Sysmex XT-2000i).

Metabolomics Profiling—Serum samples from four groups of mice ($n = 7$) were collected during euthermia, DH, arousal, and early recovery by centrifugation at 1000 × g for 10–15 min. All serum samples were frozen immediately upon collection and kept frozen until extraction. The frozen samples were shipped to Metabolon, Inc. for metabolomics profiling on their standard platform described previously (7). Briefly, the low molecular weight fractions of methanol extract were analyzed in parallel by gas chromatography and liquid chromatography in combination with mass spectrometry. Nontargeted metabolomics analyses were performed for both liquid chromatography-mass spectrometry and gas chromatography-mass spectrometry outputs, where each detected compound was identified via searching its spectral files through metabolomics libraries of about 1500 compounds at Metabolon. The data for each compound were median-centered and inter-quartile range-scaled. The company's technology platform strictly allows relative quantitation of peak areas for each metabolite. The analysis is based on the ratio changes when experimental animal groups are compared with the control animal group. All t tests are two-sided, applying a threshold of $p < 0.05$ for significance.

Glucose and Lactate Measurements—Glucose and lactate levels in erythrocytes were measured using assay kits (BioVision, Inc.). The erythrocytes were separated from serum by centrifugation, washed once in phosphate-buffered saline, and immediately frozen. Erythrocyte lysate was deproteinized by perchloric acid using a kit (BioVision, Inc). Supernatant from this extraction was used for glucose and lactate measurement. Protein levels of erythrocyte lysate were measured by a Bradford protein assay kit (Bio-Rad).

Spectral Analysis of Blood—Blood was obtained by cardiac puncture. The syringe containing the blood was frozen immediately in liquid nitrogen. To limit oxygen exposure, the thawed erythrocyte lysate was injected under a layer of paraffin oil placed in a 2-mm glass cuvette. Spectral analysis was carried out using a multiwavelength spectrophotometer HP8453 (Hewlett-Packard).

HPLC Fractionation of Adenine Nucleotides—Blood was rapidly removed from sacrificed mice and snap frozen in liquid nitrogen. Nucleotides were extracted from frozen samples using 0.4 N perchloric acid as described previously (8). Extracts were separated and quantified using reverse-phase HPLC (Waters, Millipore Corp.) on a Partissphere-bonded C$_{18}$ cartridge column at a flow rate of 1.5 ml/min. The mobile phase was 0.02 M NH$_4$H$_2$PO$_4$, pH 5.1, with a superimposed methanol gradient with the following time course: 0% for 0–4 min, 0–8% for 4–6 min, 8–20% for 6–8 min, and 20% for 8–18 min. All nucleotide and purine derivative standards were purchased from Sigma. Enzymatic confirmation of the adenylate peaks was carried out with snake venom nucleotidase and bovine ATPase treatment.

RESULTS

5′-AMP Induction of DH in Mammals—A key question raised from our earlier studies was whether 5′-AMP can be used to induce a DH state and what are the safe physiological boundaries. To investigate these issues, the effect of 5′-AMP on VO$_2$, T_b, and the importance of T_a were assessed. Mice were injected with saline or 5′-AMP (0.5 mg/g), and then placed in either T_a of 23 °C (normal husbandry temperature) or T_a of 15 °C while their VO$_2$ and T_b were simultaneously measured (Fig. 1, *a* and *b*). Mice that were given saline displayed VO$_2$
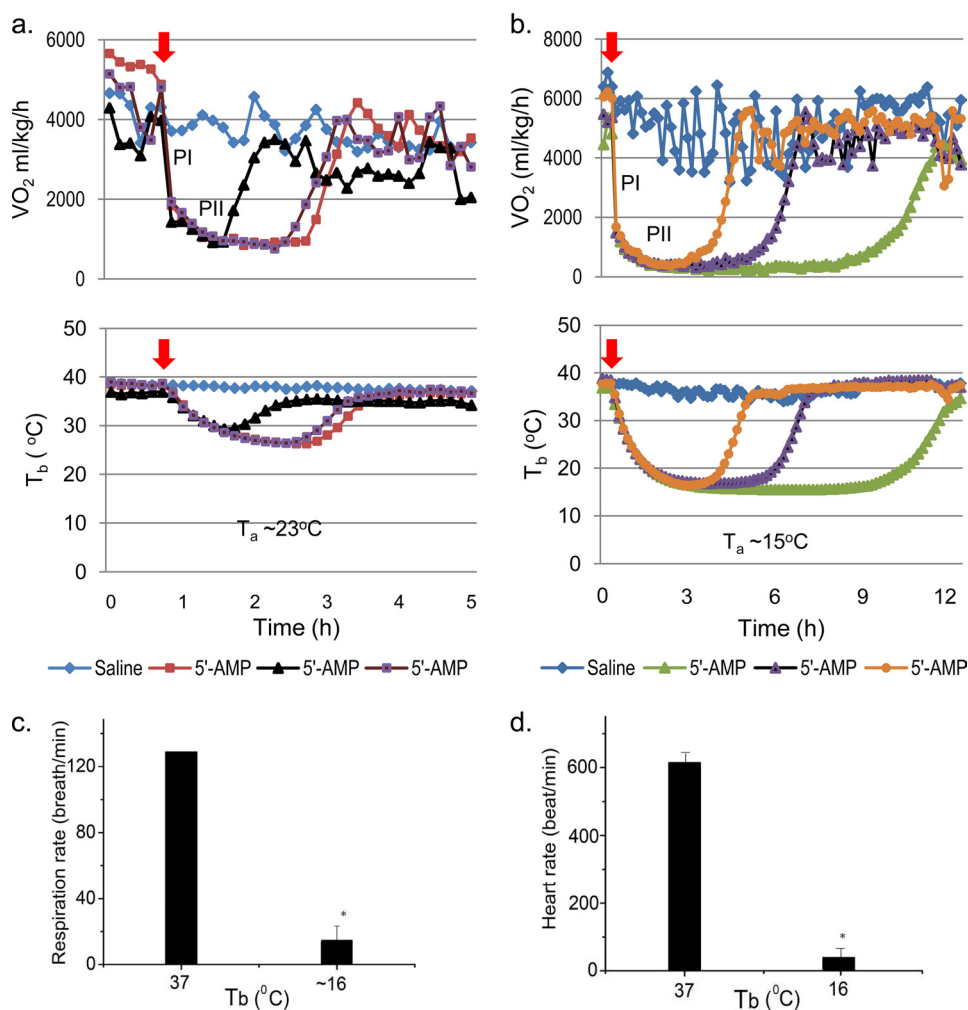
FIGURE 1. **Relationship between VO$_2$, T$_b$, and T$_a$ following 5′-AMP injection.** *a* and *b*, simultaneous measurement of T$_b$ and VO$_2$ of mice given saline or 5′-AMP (0.5 mg/g, indicated by *arrow*) in individual metabolic chambers at T$_a$ of 23 and 15 °C. Each mouse used in the study is represented by the *same color trace* for VO$_2$ and T$_b$. Sampling time for both T$_b$ and VO$_2$ was about 8 min. Note that the phase I (*PI*) decline of VO$_2$ is steep and rapid after administration of 5′-AMP. In contrast, the phase II (*PII*) VO$_2$ decline is gradual and coincides with declining T$_b$. The *colors* reflect VO$_2$ and T$_b$ of independent measurement of different animals given either saline or 5′-AMP. *c*, respiration rate of mice (*n* = 4) with T$_b$ ~16 °C compared with 37 °C. *d*, heart rate of mice (*n* = 3) with T$_b$ 16 °C compared with 37 °C. *, *p* < 0.001, paired *t* test. *Error bars*, S.E.M.

sides or backs, mice appeared to be in a state of deep stupor with outstretched limbs but were responsive to tactile stimuli. Mice kept at a T$_a$ of 23 °C did not display such behavior. Our observations indicate that mice enter DH when their T$_b$ drops below 17 °C. Mice in DH occasionally display subconscious behaviors, such as hind limb scratching, flipping and rolling on their backs, and urination (see supplemental Video 1). Maintained at a T$_a$ of 15 °C, arousal from DH occurs spontaneously for mice (Figs. 1*b* and 2 (*c* and *d*)). Once arousal was initiated, a parallel increase in VO$_2$ and T$_b$ was observed (Figs. 1*b* and 2 (*c* and *d*)). As T$_b$ rose above 22 °C, a visible shivering period ensued, followed by the return of normal mouse behaviors, such as self-grooming. Short and long term assessment of the impact of DH on mouse cognitive function by Morris water maze studies revealed no significant difference in the escape latency of the animals after undergoing DH treatment (data not shown). Both male and female mice showed equal ability to enter DH. Rats and dogs given 5′-AMP and cooled to T$_b$ of 18–20 °C (rats) and 20–22 °C (dogs) displayed a similar ability to undergo DH (see supplemental Fig. 2, *a* and *b*). Together, these observations demonstrate that 5′-AMP can be used to initiate reversible DH of mammals.

5′-AMP Dosages Initiate but Do Not Control the Length of DH—Next, we examined the concentration dependence of 5′-AMP in mediating the process of DH in mice. Five groups of mice were injected with saline or 5′-AMP doses ranging from 0.1 to 1.0 mg/g and then kept at a T$_a$ of 15 °C. Our findings demonstrate that the concentration of 5′-AMP is important for entering into DH (Figs. 1*b* and 2 (*a–d*)). Lower dosages of 5′-AMP did not produce DH but instead a transient hypometabolic state with a moderate decrease in T$_b$ (Fig. 2*b*). Surprisingly, increasing the dosage of 5′-AMP from 0.1 to 1 mg/g did not alter the phase I VO$_2$ decline (Figs. 1*b* and 2 (*b–d*)). Comparing the T$_b$ and VO$_2$ profiles of mice revealed an aborted phase II when mice failed to enter DH (Fig. 2*b*). However, once DH was attained, there was considerable overlap in spontaneous arousal time between the different dosages of 5′-AMP administered (Figs. 1*b* and 2 (*c* and *d*)).

We further investigated whether other nucleoside monophosphates, such as cytidine monophosphate (5′-CMP) or guanosine

levels ranging between 4000 and 6500 ml/kg/h regardless of whether T$_a$ was 15 or 23 °C. The T$_b$ of these mice measured by telemetry remained at about 37 °C. In contrast, about 10 min after 5′-AMP administration, the phase I VO$_2$ had dropped steeply to below 2000 ml/kg/h for both groups of mice at T$_a$ of 23 or 15 °C. Notably, T$_b$ of the mice dropped only slightly over the same period. The phase II VO$_2$ decline that followed corresponded with the major decline in T$_b$. For mice kept at a T$_a$ of 23 °C, the phase II decline reached a nadir of about 1000 ml/kg/h and a T$_b$ of 26–28 °C (Fig. 1*a*; also see supplemental Fig. 1). After about 2 h in the hypometabolic state, euthermic T$_b$ and VO$_2$ levels were restored. For mice kept at a T$_a$ of 15 °C, the phase I response was similar to that of animals kept at 23 °C; however, their phase II decline was longer and deeper, reaching a nadir at about 300 ml/kg/h and a T$_b$ of about 16 °C (Fig. 1*b*; also see supplemental Fig. 1). Normal respiration rates of mice were reduced from ~120 to ~10 breaths/min (Fig. 1*c*). In addition, heart rates were similarly reduced from ~600 to about 50 beats/min (Fig. 1*d*). When laid on their
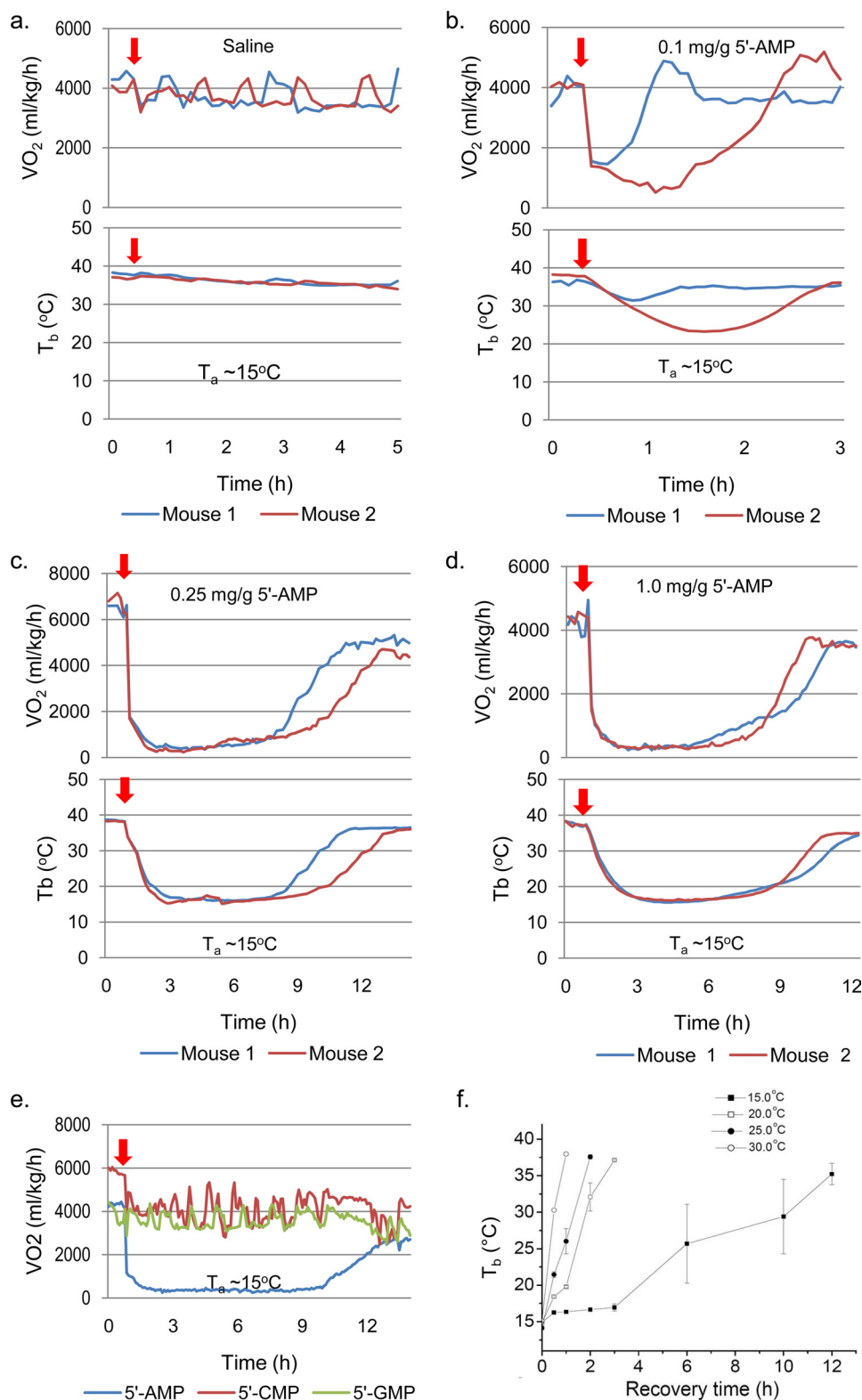
FIGURE 2. **DH as a function of 5'-AMP dosage.** *a–d*, simultaneous measurement of T_b and VO_2 of mice given different dosages of 5'-AMP and maintained at T_a of 15 °C. The different *colors* in the *graph* reflect VO_2 and T_b of different animals used in the study. *e*, comparison of VO_2 levels in mice given a similar amount (0.5 mg/g) of either 5'-AMP, 5'-CMP, or 5'-GMP. *f*, arousal from DH and the rise in T_b of mice ($n = 4$) maintained at various T_a values.

The effect of T_a on the arousal rate from DH was investigated. Mice in DH were kept at different T_a, and the time required for T_b to return to 37 °C was measured (Fig. 2*f*). An increase in T_a led to a faster recovery rate. These observations indicated that the appropriate T_a plays a major role in maintaining DH. However, differential arousal times at a constant T_a indicate the involvement of an endogenous control that remains unclear. Suppression of arousal by additional injections of 5'-AMP or a further decrease in T_a to less than 13 °C resulted in increased fatalities. Together, these studies indicate that the phase I VO_2 response to 5'-AMP was not dependent on the T_a or the T_b of the animal. However, the phase II VO_2 decline is associated with declining T_b of the animal and is moderated by T_a. Once the animal enters DH under a constant T_a, the arousal time is spontaneous and has no apparent relationship to the dose of 5'-AMP administered.

Dephosphorylation of 5'-AMP to Adenosine Is Not Essential for DH—Circulating 5'-AMP is dephosphorylated to adenosine by the membrane-bound extracellular enzyme ecto-5'-nucleotidase/CD73 (9). Therefore, CD73$^{-/-}$ mice were used to investigate whether blocking 5'-AMP dephosphorylation affects the animal's hypometabolic responses to 5'-AMP. No differential VO_2 response was observed between ecto-5'-nucleotidase/CD73-deficient and wild type mice given 5'-AMP (Fig. 3*a*). Next we investigated whether ecto-5'-nucleotidase/CD73-deficient mice have a differential response to lower dosages of 5'-AMP. A cooling regime of T_a at 4 °C for 1 h was used to determine the lowest effective dosage to reduce T_b into the DH range. Using this cooling regime, a 5'-AMP dose of 0.125 mg/g was able to induce DH in the majority of ecto-5'-nucleotidase/

monophosphate (5'-GMP), could produce a similar hypometabolic response in mice. Unlike the 5'-AMP-injected animals, mice given 5'-CMP or 5'-GMP (0.5 mg/g) displayed normal VO_2 and activity throughout the study (Fig. 2*e*).

CD73-deficient mice but was mostly unsuccessful in wild type animals (Fig. 3*b*). These observations suggest that the presence of ecto-5'-nucleotidase/CD73 in wild type mice reduces the effectiveness of lower doses of 5'-AMP to induce DH.
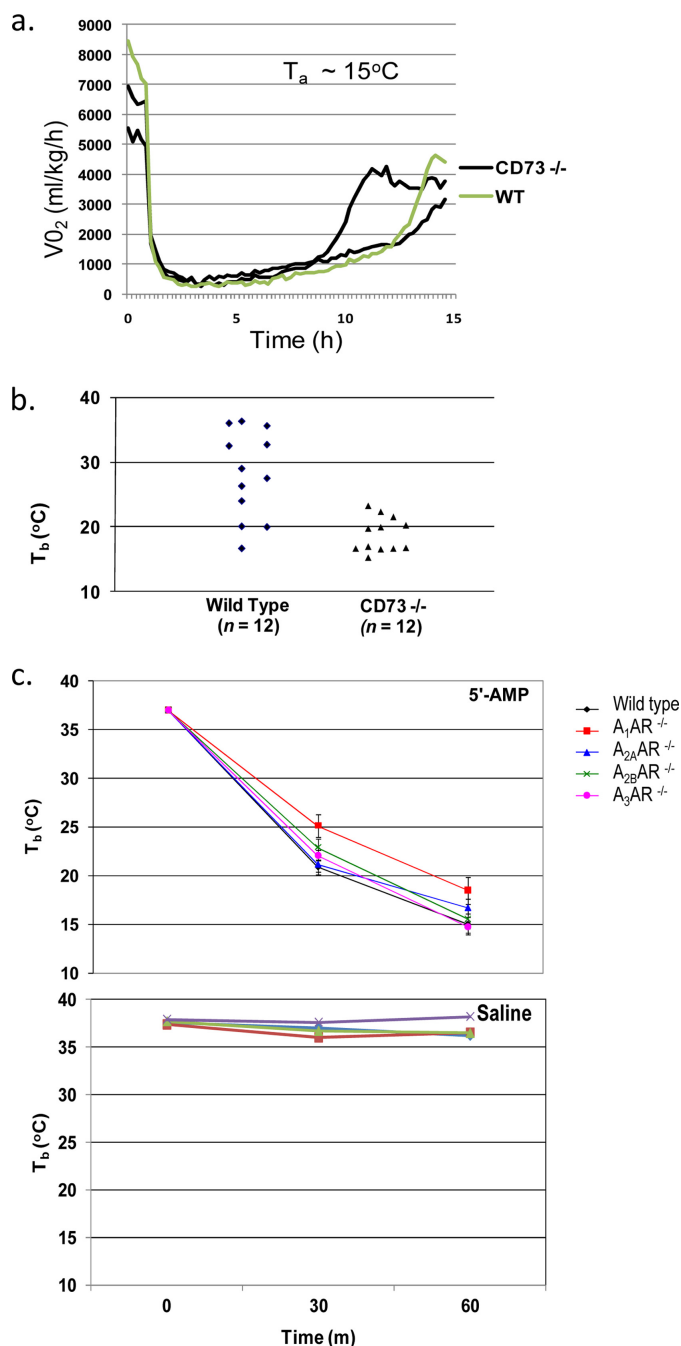
a.

b.

c.

FIGURE 3. **Loss of adenosine receptors or ecto-5′-nucleotidase deficiency does not block DH by 5′-AMP.** *a*, the VO_2 profiles of ectonucleotidase/CD73-deficient ($n = 2$) and wild type mice following 5′-AMP (0.5 mg/g) administration. *b*, individual T_b of ectonucleotidase/CD73-deficient and wild type mice ($n = 12$) after 1 h at 4 °C T_a with injection of 0.125 mg/g 5′-AMP. *c, top*, T_b time course of mice ($n = 4$) with the adenosine receptor genotype $A_1^{-/-}$, $A_{2a}^{-/-}$, $A_{2b}^{-/-}$, or $A_3^{-/-}$ or wild type were given 0.5 mg/g 5′-AMP after 1 h at 4 °C T_a. *Bottom*, T_b of mice of the same genotype given saline after 1 h at 4 °C T_a. *Error bars*, S.E.M.

The role played by adenosine receptors in DH was investigated using mice genetically engineered for adenosine receptor deficiency (10–13). Mice deficient in A_1, A_{2A}, A_{2B}, or A_3 adenosine receptors were compared with wild type animals for their response to 5′-AMP or saline. A similar cooling regime as above was used. Based on T_b, all of the different adenosine receptor-deficient and wild type mice showed equal ability to enter DH

(Fig. 3*c*). Mice of the same genotype given saline did not change their T_b under a similar cooling regime.

Together, these findings demonstrate that neither the dephosphorylation of 5′-AMP into adenosine nor the presence of adenosine receptor-mediated processes is essential for 5′-AMP mediated hypometabolism.

DH Is Associated with Elevated Levels of 2,3-Bisphosphoglycerate—To gain biochemical insight into the fate and effects of 5′-AMP, we undertook a metabolomics analysis of serum metabolites from mice during the states of euthermia (preinjection), DH, at arousal and at early recovery. Liquid and gas chromatography and mass spectrometry analysis of the serum revealed that the level of 5′-AMP at DH (about 3 h postinjection) and arousal was less than 1.5-fold that observed in euthermic mice, indicating that the majority of the administered 5′-AMP had been catabolized. This conclusion is supported by the large increase in purine catabolites, including inosine, xanthine, xanthosine, hypoxanthine, urate, and allantoin during DH (Table 1). At early recovery, the majority of these purine catabolites had returned to levels observed in the preinjected animals (euthermia) except allantoin, an end product of purine catabolism in mice. A 2-fold increase in ADP over that of the euthermic state was observed during DH. The levels of adenosine during DH and arousal were lower during euthermia, suggesting that 5′-AMP was primarily catabolized through the AMP deaminase pathway.

Metabolomics studies further revealed a higher level of 2,3-BPG in DH than euthermic state (data not shown). The enzyme that catalyzes 2,3-BPG biosynthesis from 1,3-BPG, bisphosphoglycerate mutase, is found only in erythrocytes and placenta (14). The observed increase in 2,3-BPG implicates erythrocytes as the source of 2,3-BPG and a likely cellular target of 5′-AMP. A time course assay of 2,3-BPG in erythrocytes revealed a rapid increase shortly after 5′-AMP administration to mice (Fig. 4*a*).

The large increase in 2,3-BPG levels could be an indicator of reduced glycolysis in the erythrocytes. Therefore, the levels of glucose and lactate in the erythrocytes obtained from 5′-AMP-treated and untreated mice were measured. Our analysis revealed that the level of glucose in the erythrocytes of 5′-AMP treated mice was over 3 times higher and the level of lactate was about 2 times lower than those from untreated animals (Fig. 4, *b* and *c*). Together, these findings suggest that the increase in 2,3-BPG levels was probably linked to reduce glucose utilization in the erythrocytes of 5′-AMP-treated mice.

Uptake of 5′-AMP by Erythrocytes and Elevated Levels of Deoxyhemoglobin—To verify whether 5′-AMP was directly taken up by erythrocytes, we incubated freshly isolated wild type mouse erythrocytes with radiolabeled [^{14}C]adenosine or 5′-[^{14}C]AMP. Using TLC, the catabolic and salvage products from [^{14}C]adenosine or 5′-[^{14}C]AMP were identified shortly after their addition to erythrocytes *in vitro*. Uptake of adenosine into erythrocytes occurred very rapidly as observed previously (15). TLC analysis showed that uptake of [^{14}C]adenosine was primarily salvaged to form 5′-[^{14}C]AMP and [^{14}C]ADP (Fig. 5*a*). This would be consistent with previous observations that adenosine in erythrocytes is salvaged by adenosine kinase into 5′-AMP and then via adenylate kinase into ADP (16–18). Erythrocytes also displayed rapid uptake of 5′-[^{14}C]AMP that

TABLE 1

Relative levels of purine intermediates in serum that showed significant alteration during euthermia, deep hypometabolism, arousal, and early recovery

For each group, the relative quantization value of each metabolite is the average obtained from seven mice. For each of the metabolites, the average euthermia control value is arbitrarily set at 1. The -fold change in DH, arousal, and early recovery is relative to the value obtained for euthermia. The probability that the changes were due to random factors is quantified by the p values, and the false positive rate is quantified by q values of t tests that are shown in italic type. (Note that for the data points with missing values, no acceptable measurement for that compound was obtained for the group.)

| Altered purine metabolites ($n = 7$)	DH/Euthermia			Arousal/Euthermia			Early recovery/Euthermia		
	-Fold change	p value	q value	-Fold change	p value	q value	-Fold change	p value	q value
Xanthine	8.83	*0.000*	*0.001*	4.97	*0.012*	*0.007*	1.13	*0.356*	*0.127*
Xanthosine	11.8	*0.000*	*0.000*	2.82	*0.004*	*0.003*	1.03	*0.793*	*0.227*
Hypoxanthine	8.69	*0.004*	*0.005*	3.07	*0.033*	*0.017*			
Inosine	4.91	*0.026*	*0.021*	1.30	*0.351*	*0.115*			
Adenosine	0.66	*0.004*	*0.005*	0.41	*0.033*	*0.017*	0.61	0.523	0.166
5′-AMP	1.21	*0.026*	*0.021*	1.44	*0.351*	*0.115*	0.92	0.587	0.178
ADP	1.79	*0.021*	*0.019*	2.02	*0.004*	*0.003*	0.95	*0.807*	*0.228*
Urate	3.3	*0.001*	*0.001*	2.70	*0.002*	*0.002*	1.57	*0.144*	*0.064*
Allantoin	15.3	*0.000*	*0.000*	18.16	*0.000*	*0.000*	13.44	*0.000*	*0.000*
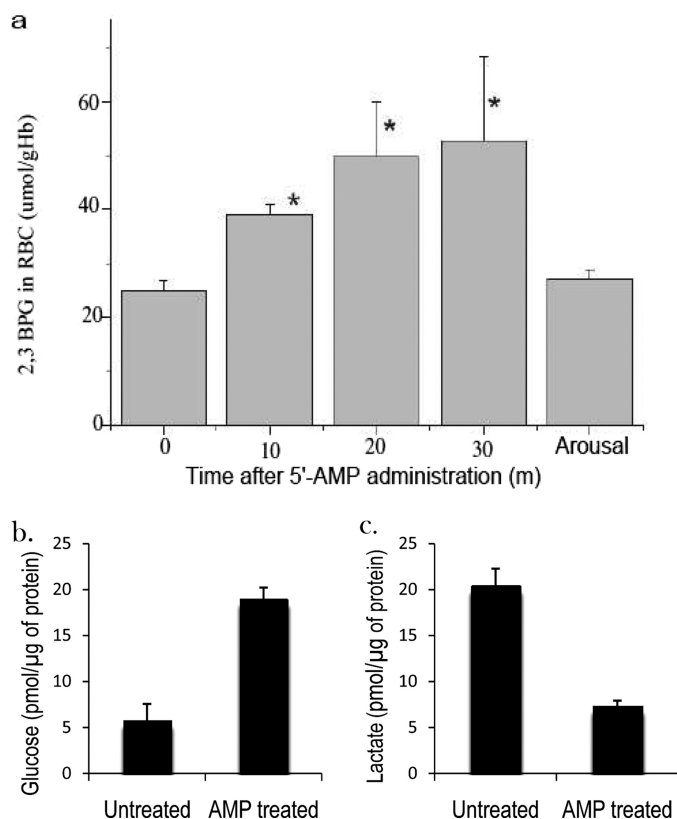
FIGURE 4. **Increased production of 2,3-bisphosphoglycerate induced by 5′-AMP uptake by erythrocytes.** *a*, levels of 2,3-bisphosphoglycerate in erythrocytes/red blood cells (*RBC*) obtained from mice after administration of 5′-AMP (*, data shown as mean ± S.E.M. (*error bars*), $p < 0.05$, $n = 6$). *b* and *c*, glucose and lactate levels in erythrocytes isolated from 5′-AMP and untreated mice (data shown as mean ± S.E.M. $p < 0.01$, $n = 4$).

drives the formation of [14C]ADP (Fig. 5*a*). No increase in [14C]ATP was observed, which is consistent with the adenylate equilibrium (ATP + 5′-AMP ↔ 2ADP) favoring the forward direction toward ADP driven by the influx of 5′-AMP. To expand on these observations, metabolite extracts were made from whole blood of mice during the states of euthermia and DH and at arousal. HPLC analysis revealed that extracts obtained from DH displayed a significant increase in purine catabolites, including inosine and uric acid (Fig. 5, *b–e*). The uptake of 5′-AMP into erythrocytes resulted in a significant rise in intracellular ADP and a corresponding drop in ATP levels.

This change in the adenylate ratio is supported by observations that an additional injection of 5′-AMP during DH further increased ADP at the expense of ATP levels while also causing a large increase in inosine (Fig. 5*e*).

Because 2,3-BPG allosterically inhibits hemoglobin affinity for oxygen, an increase in the levels of deoxyhemoglobin is predicted. Blood high in deoxyhemoglobin has a signature absorbance peak at 760 nm (19). In addition, oxyhemoglobin has a weaker absorbance than deoxyhemoglobin at 660 nm (20). Spectral analysis of blood from the 5′-AMP-treated mice displayed a signature peak absorbance at 760 nm. It also had a higher absorbance at 660 nm than blood obtained from untreated animals (Fig. 5*f*). These studies demonstrate that 5′-AMP uptake by the erythrocytes triggers the biochemical response that leads to an increase of 2,3-BPG, which in turn decreases hemoglobin affinity for oxygen.

DISCUSSION

Mice deficient in ectonucleotidase/CD73 or adenosine receptors enter DH with an efficiency similar to that of wild type animals. These two complementary but independent mouse genetic experiments demonstrate that dephosphorylation of 5′-AMP into adenosine was apparently not essential for DH. Our investigations revealed that unlike 5′-AMP-injected mice, the 5′-CMP- and 5′-GMP-injected mice did not show a decrease in VO2 levels. Because adenosine and adenylate nucleotides can be converted to 5′-AMP *in vivo*, administration of adenosine or adenylate nucleotides induces a transient decrease of VO2 in mice. Due to adenosine's low aqueous solubility and half-life of less than 10 s in plasma, DH of mice under similar conditions was not observed (see supplemental Fig. 3*a*). Unlike the rapid drop observed for 5′-AMP following its administration, other adenylate nucleotides, including cAMP, displayed a more gradual decline in VO2 (supplemental Fig. 3, *b* and *c*; data not shown). We surmised that the slower response is consistent with the breakdown of cAMP to 5′-AMP by phosphodiesterases; however, the concentration of 5′-AMP generated from cAMP did not reach the levels required for DH to take hold. A slower VO2 response was also observed for ADP and ATP given at similar concentration (data not shown).

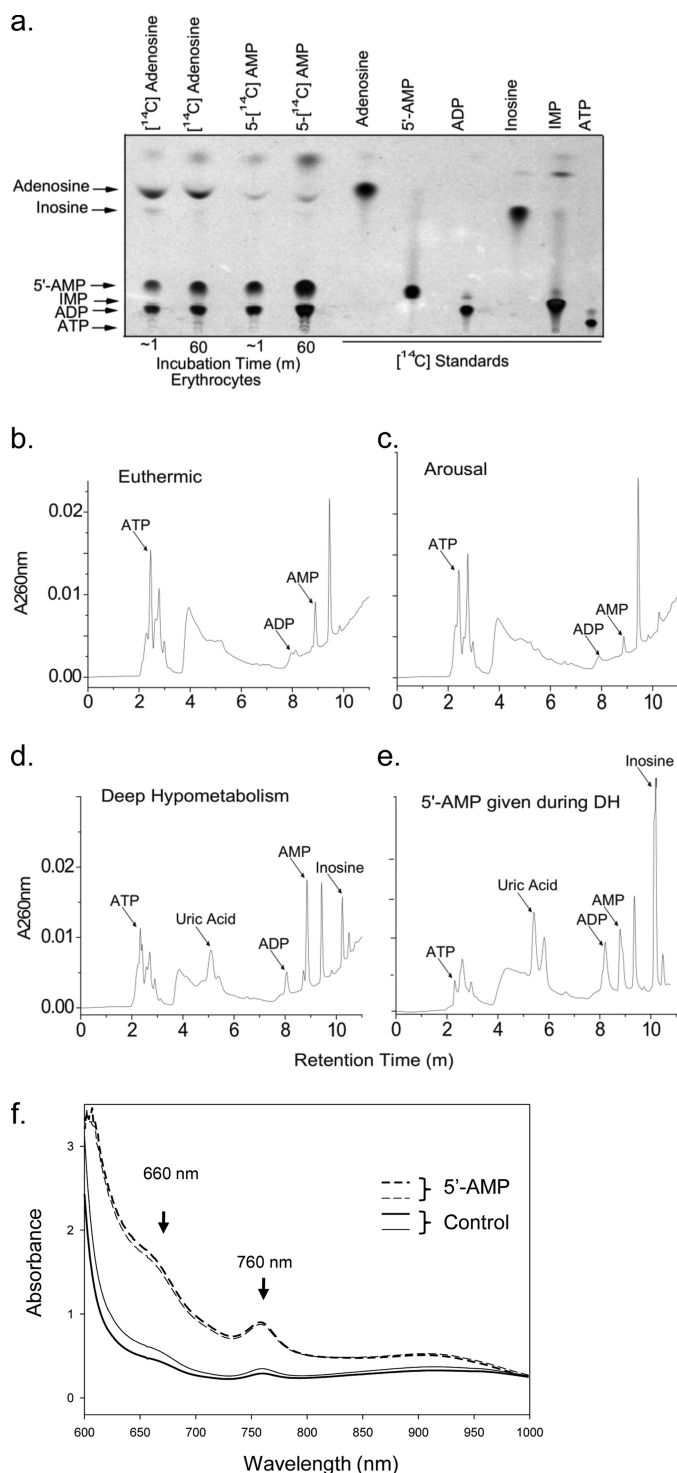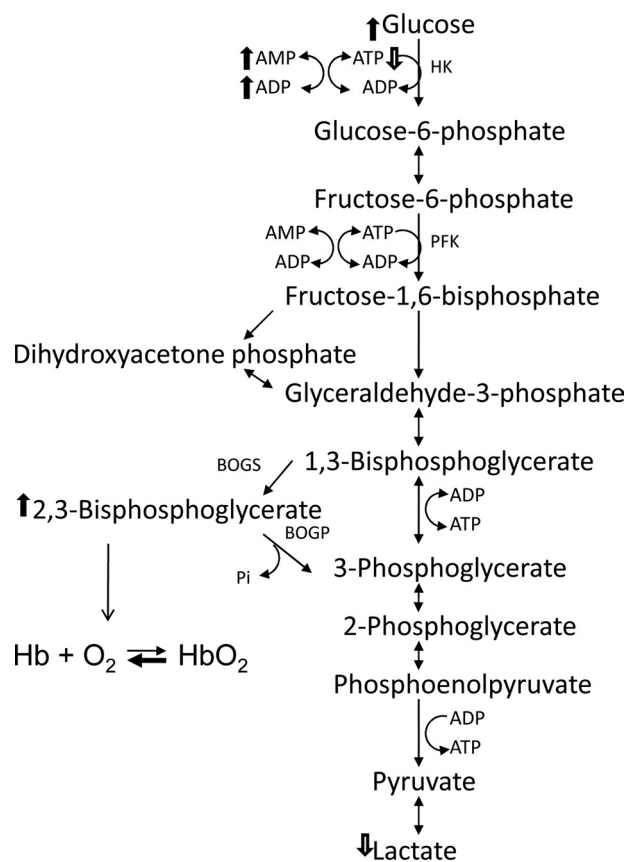Previous studies have shown that 5′-[11C]AMP cannot cross the blood brain barrier (16). Rather, the radiotracer

FIGURE 6. **A proposed model for 5'-AMP-mediated hypometabolism via erythrocytes.** The model indicates altered levels of glycolytic intermediates and adenylates observed. In the erythrocytes, uptake of 5'-AMP drives the production of ADP at the expense of ATP. In turn, glycolytic steps dependent on ATP at hexokinase (*HK*) were slowed, resulting in the buildup of glucose and decreased production of lactate. The reduction in glycolytic rate will drive the production of 2,3-BPG from 1,3-BPG by the enzyme bisphophoglycerate mutase to stabilize intracellular ATP levels. The increase in 2,3-BPG allosterically reduces the affinity of hemoglobin (*Hb*) for oxygen, which could explain the rapid and steep decline in VO₂ illustrated by phase I and increased deoxyhemoglobin levels.

FIGURE 5. **Uptake of 5'-AMP by erythrocytes and increased deoxyhemoglobin levels.** *a*, uptake of radiolabeled [14C]adenosine or 5'-[14C]AMP by isolated erythrocytes *in vitro*. Autoradiograph showing the TLC analysis of erythrocyte extracts compared with known radiolabeled purine standards. Shown are representative HPLC chromatograms of purine products extracted from blood obtained from mice in euthermia (*b*), in spontaneous arousal (*c*), and during DH (*d*) and an animal in DH given a second injection of 0.5 mg/g 5'-AMP and sacrificed 2 h later (*e*). HPLC of purine standards was used to determine the identity of the various peaks. *f*, absorbance spectrum of whole blood from mice (n = 2) treated with 5'-AMP (*dashed lines*) or untreated (*solid lines*). Blood was taken 10 min after intraperitoneal administration of 5'-AMP (0.5 mg/g).

was found primarily in red blood cells and in two highly perfused organs, lung and heart. In the blood, the uptake of 5'-[11C]AMP was observed to alter the ADP/ATP ratio, as predicted by the adenylate equilibrium (16). Our studies demonstrate that 5'-[14C]AMP was taken up rapidly by erythrocytes from wild type and CD73⁻/⁻ mice. TLC analysis revealed that the uptake of 5'-AMP into erythrocytes drives the production of ADP. In addition, our HPLC analysis revealed that uptake of 5'-AMP by erythrocytes alters the relative levels of ADP and ATP, which is consistent with the adenylate equilibrium. We propose that the influx of 5'-AMP into erythrocytes drives the adenylate equilibrium (ATP + 5'-AMP ↔ 2ADP) to increase ADP production, utilizing intracellular ATP (Fig. 6). The first step of glycolysis carried out by hexokinase (glucose to glucose 6-phosphate) requires ATP to proceed (21). Our studies demonstrate that glucose is highly elevated, but lactate is decreased during DH, which is consistent with a reduced level of glycolysis. Metabolic modeling studies have demonstrated that the production of 2,3-BPG from 1,3-BPG is enhanced when glycolysis slows as a response to stabilize ATP levels in the erythrocytes (22). A small change

in ATP levels can have a large effect on 2,3-BPG production in erythrocytes (22).

In erythrocytes, 2,3-BPG regulates the affinity of hemoglobin for oxygen in an allosteric manner (21). The affinity of 2,3-BPG for deoxygenated hemoglobin is very high, but it binds only weakly to oxygenated hemoglobin (21, 22). Thus, a rise in 2,3-BPG in the erythrocyte following 5′-AMP administration would lower its ability to transport oxygen. The phase I VO_2 profile could reflect a reduced rate of oxygen transport by the erythrocytes rather than a sudden shutdown of the animal's metabolic rate. This is supported by the observation that the amplitude of the phase I decline in VO_2 was very similar over a wide dosage range of 5′-AMP, an observation consistent with allosteric regulation. In addition, blood from mice given 5′-AMP has much higher deoxyhemoglobin levels than blood from untreated animals. We propose that an allosteric suppression of hemoglobin's affinity for oxygen by 2,3-BPG results in delivery of less oxygen to organs, and this in turn triggers a physiological adaption to decrease overall metabolic activity *in vivo*. When the body's heat loss to the environment is greater than that generated endogenously, the T_b will decline toward the T_a. As T_b drops, the overall demand for oxygen also decreases, thereby creating an interdependent loop between T_b and VO_2, which is consistent with the observed phase II VO_2 and T_b profiles. If maintained at the appropriate T_a, the animal's T_b will attain an equilibrium between the energy released by reduced metabolic activity and the heat loss to the environment, thereby allowing the animal to maintain DH. Gradual rewarming of the animal, leading to increased VO_2, triggers arousal from DH. However, the regulation of arousal remains complex because mice arouse at vastly different times even when T_a remains constant.

Metabolic inhibitors, such as 2-deoxyglucose and hydrogen sulfide (H_2S), are able to induce torpor and "suspended animation" of small mammals (23, 24). How these metabolic inhibitors achieve reduced T_b is currently unclear. However, the effects of these inhibitors on erythrocyte functions are well established. Inhaled H_2S gas is metabolized by erythrocytes into reactants ($HbO_2 + 2H_2S \rightarrow 2S + Hb + H_2O$) that would deplete oxyhemoglobin levels (25). Erythrocytes lack mitochondria and are unable to carry out β-oxidation. Therefore, inhibitors of β-oxidation, such as mercaptoacetate, do not disrupt erythrocyte ATP production and therefore do not induce torpor of hamsters (23). However, inhibition of hexokinase, the first enzymatic step of glycolysis, by 2-deoxyglucose would severely impact the ability of erythrocytes to produce ATP. In addition, hypothermia of mammals can be induced by exsanguination, a process in which a large volume of blood is removed from the body (3, 26). Furthermore, hypothermia is a documented response to prolonged hypoxia (4). Together, these findings suggest that erythrocytes could be a common target for the various agents known to induce hypometabolism in mammals. In summary, we have demonstrated a method using a natural metabolite, 5′-AMP, together with the appropriate T_a, to initiate, maintain, and terminate DH of diverse species of mammals.

REFERENCES

1. Heldmaier, G., Ortmann, S., and Elvert, R. (2004) *Respir. Physiol. Neurobiol.* **141,** 317–329
2. Simpkins, C. E., Montgomery, R. A., Hawxby, A. M., Locke, J. E., Gentry, S. E., Warren, D. S., and Segev, D. L. (2007) *Am. J. Transplant.* **7,** 99–107
3. Ikeda, S. (1965) *Tohoku J. Exp. Med.* **87,** 185–198
4. Wood, S. C. (1991) *Annu. Rev. Physiol.* **53,** 71–85
5. Zhang, J., Kaasik, K., Blackburn, M. R., and Lee, C. C. (2006) *Nature* **439,** 340–343
6. Overton, J. M., and Williams, T. D. (2004) *Physiol. Behav.* **81,** 749–754
7. Lawton, K. A., Berger, A., Mitchell, M., Milgram, K. E., Evans, A. M., Guo, L., Hanson, R. W., Kalhan, S. C., Ryals, J. A., and Milburn, M. V. (2008) *Pharmacogenomics* **9,** 383–397
8. Knudsen, T. B., Winters, R. S., Otey, S. K., Blackburn, M. R., Airhart, M. J., Church, J. K., and Skalko, R. G. (1992) *Teratology* **45,** 91–103
9. Thompson, L. F., Eltzschig, H. K., Ibla, J. C., Van De Wiele, C. J., Resta, R., Morote-Garcia, J. C., and Colgan, S. P. (2004) *J. Exp. Med.* **200,** 1395–1405
10. Chen, J. F., Huang, Z., Ma, J., Zhu, J., Moratalla, R., Standaert, D., Moskowitz, M. A., Fink, J. S., and Schwarzschild, M. A. (1999) *J. Neurosci.* **19,** 9192–9200
11. Salvatore, C. A., Tilley, S. L., Latour, A. M., Fletcher, D. S., Koller, B. H., and Jacobson, M. A. (2000) *J. Biol. Chem.* **275,** 4429–4434
12. Sun, D., Samuelson, L. C., Yang, T., Huang, Y., Paliege, A., Saunders, T., Briggs, J., and Schnermann, J. (2001) *Proc. Natl. Acad. Sci. U.S.A.* **98,** 9983–9988
13. Csóka, B., Németh, Z. H., Virág, L., Gergely, P., Leibovich, S. J., Pacher, P., Sun, C. X., Blackburn, M. R., Vizi, E. S., Deitch, E. A., and Haskó, G. (2007) *Blood* **110,** 2685–2695
14. Pritlove, D. C., Gu, M., Boyd, C. A., Randeva, H. S., and Vatish, M. (2006) *Placenta* **27,** 924–927
15. Noji, T., Karasawa, A., and Kusaka, H. (2004) *Eur. J. Pharmacol.* **495,** 1–16
16. Mathews, W. B., Nakamoto, Y., Abraham, E. H, Scheffel, U., Hilton, J., Ravert, H. T., Tatsumi, M., Rauseo, P. A., Traughber, B. J., Salikhova, A. Y., Dannals, R. F., Wahl, R. L. (2005) *Mol. Imaging Biol.* **7,** 203–208
17. Tsuboi, K. K., and Chervenka, C. H. (1975) *J. Biol. Chem.* **250,** 132–140
18. Hawkins, C. F., and Bagnara, A. S. (1987) *Biochemistry* **26,** 1982–1987
19. Chance, B., Leigh, J. S., Miyake, H., Smith, D. S., Nioka, S., Greenfeld, R., Finander, M., Kaufmann, K., Levy, W., and Young, M. (1988) *Proc. Natl. Acad. Sci. U.S.A.* **85,** 4971–4975
20. Shepherd, A. P., Sutherland, J. C., and Wilson, A. F. (1975) *J. Appl. Physiol.* **39,** 152–155
21. Lehninger, A. (1982) *Principles of Biochemistry*, 2nd Ed., W. H. Freeman, New York
22. Mulquiney, P. J., and Kuchel, P. W. (1999) *Biochem. J.* **342,** 597–604
23. Dark, J., Miller, D. R., and Zucker, I. (1994) *Am. J. Physiol.* **267,** R496–R501
24. Blackstone, E., Morrison, M., and Roth, M. B. (2005) *Science* **308,** 518
25. Evans, C. L. (1967) *Q. J. Exp. Physiol. Cogn. Med. Sci.* **52,** 231–248
26. Rhee, P., Talon, E., Eifert, S., Anderson, D., Stanton, K., Koustova, E., Ling, G., Burris, D., Kaufmann, C., Mongan, P., Rich, N. M., Taylor, M., and Sun, L. (2000) *J. Trauma* **48,** 439–447; discussion 447–450